

Critical behavior of the Baxter-Wu model with quenched impurities

M. A. Novotny and D. P. Landau

Department of Physics and Astronomy, University of Georgia, Athens, Georgia 30602

(Received 2 March 1981)

We have used an importance-sampling Monte Carlo technique to study the Baxter-Wu model with various fractions of the lattice sites occupied by random, quenched, nonmagnetic, site impurities. We found the system had long-time fluctuations which were caused by the creation and motion of domain boundaries. For this reason our study required the use of a large number of Monte Carlo steps per spin. The data were analyzed using finite-size scaling to extract the infinite-lattice critical exponents and critical amplitudes from the Monte Carlo simulation of finite lattices. This analysis of the data for the pure Baxter-Wu model yielded results which agreed well with exact results and series-expansion predictions. The addition of quenched site impurities caused a dramatic change in the critical behavior. The pure-lattice critical exponents ($\nu = \frac{2}{3}$, $\alpha = \frac{2}{3}$, $\gamma_m \approx 1.17$) change upon the addition of only a few percent impurities to $\nu = 1.00 \pm 0.07$, $\alpha \leq 0.0$, and $\gamma_m = 1.95 \pm 0.08$. The phase diagram as a function of impurity concentration and an estimate for the infinite-lattice percolation limit are also given.

I. INTRODUCTION

The effects of impurities on the critical behavior of simple magnetic models are not only of great intrinsic interest but also provide a bridge which spans the gap between theoretical and physical systems. We now know that the modification of the critical behavior owing to the addition of impurities depends on the type of impurity. The critical behavior of systems with annealed (mobile) impurities is related to the corresponding pure-lattice properties through a set of renormalized critical exponents.^{1,2} The more interesting and more difficult question of the effects which quenched (fixed) impurities have on the critical behavior of systems has been studied by various methods on several types of models. Exact work³ on a rectangular Ising model with various types of quenched, *periodic* point defects proved that the critical temperature, but not the critical exponents, depended on the impurity concentration. McCoy and Wu showed⁴ that, for an Ising square lattice with uniform bonds in one direction and quenched, random bonds in the remaining direction, the transition is smeared out. Series-expansion studies on systems with random, quenched impurities gave estimates^{5,6} for the dependence of T_c on the impurity concentration but were not able to estimate the critical exponents accurately enough to determine if they depend upon the impurity concentration. Using general arguments, Harris suggested⁷ that when random, quenched impurities are added to a system with a negative specific heat exponent α , the critical temperature but not the critical behavior will change. If α is positive, however, Harris predicted new critical behavior might occur but only within a critical region

of temperature about $T_c(x)$ on the order of $x^{1/\alpha}$ where x is the fraction of quenched nonmagnetic impurities present.⁸ Renormalization-group theory has been used to study an m -component continuous-spin model with random, quenched impurities⁹⁻¹⁴ and has shown that if the original system has a positive α a new "random" fixed point is stable. The critical exponents may then change, but, since ϵ -expansion results are available only to $O(\epsilon)$, it is unclear how reliable the exponent estimates are. A real-space renormalization-group method using a Migdal-Kadanoff approximate recursion relation has been used¹⁵ to study the bond-dilute two-dimensional (2D) Ising model and gives a phase diagram in quantitative agreement with known results. However, when applied to the pure Ising model, the critical exponents obtained by this method vary substantially from the exact exponents. Monte Carlo simulations for two-dimensional Ising models¹⁶⁻¹⁸ with quenched site impurities have found no evidence for changes in critical behavior. However, since $\alpha = 0$ for these models, it is unclear if any change should be expected. Monte Carlo studies of the simple cubic Ising model¹⁹ ($\alpha \approx 0.12$) have also not observed any change in the critical exponents with the addition of quenched site impurities. However for this model the predicted width of the "impure critical region" is probably too small to be observable for lattice sizes amenable to study by Monte Carlo techniques. For example, if $x = 0.2$ then $x^{1/\alpha} \sim 10^{-6}$. We have chosen to study the effects of quenched impurities on the Baxter-Wu²⁰ model for which $\alpha = \frac{2}{3}$ since the "impure critical region" should be observable using Monte Carlo methods; if $x = 0.2$ then $x^{1/\alpha} \sim 0.1$.

We have previously described preliminary results

for the site-impure Baxter-Wu model.²¹ In Sec. II we will describe the details of our simulations and shall present the results in Sec. III. In Sec. IV we shall analyze the critical behavior obtained for a wide range of temperatures and impurity concentrations. Section V will summarize our conclusions.

II. MODEL AND METHOD

A. Baxter-Wu model

The Baxter-Wu model²⁰ is a simple Ising model with three-body interactions. It is defined on a triangular lattice with the Hamiltonian given by

$$\mathcal{H} = -J \sum \sigma_i \sigma_j \sigma_k, \quad (1)$$

where $\sigma_i = \pm 1$ and the sum is over all triangles made up of nearest-neighbor spins on the lattice. In the absence of an external field the ground state of this model is fourfold degenerate. The triangular lattice can be broken into three interpenetrating sublattices, and the single ferromagnetic ground state has all spins up while the three ferrimagnetic ground states have the spins on one sublattice up and the spins on the other two sublattices down (see Fig. 1). An exact solution by Baxter and Wu²⁰ for the pure system (where the fraction of lattice sites occupied by non-magnetic impurities is $x = 0$) gives the critical temperature $kT_c(0)/J = 2/\ln(\sqrt{2} + 1) \approx 2.2692$ and the critical exponents $\alpha = \alpha' = \nu = \nu' = \frac{2}{3}$. Series-expansion results give the magnetic susceptibility

$\gamma'_M \approx 1.17$,^{22,23} and a conjecture for the spontaneous magnetization²³ M gives $\beta_M = \frac{1}{12}$.

The Baxter-Wu model has two order parameters. The magnetic order parameter m is related to the spontaneous magnetization M of the infinite system at temperatures below T_c . A second order parameter p is related to the spontaneous polarization²³ P of the infinite lattice Baxter-Wu model. The polarization can be regarded as the response of dipoles formed by adjacent pairs of spins to an applied electric field. A study of the low-temperature series expansion has led to a conjecture²³ for P that gives the critical exponent for the polarization $\beta_P = \frac{1}{12}$. The conjectures for the two order parameters predict²³ that the critical amplitudes should have the ratio $B_M/B_P = 3/2\sqrt{2} \approx 1.06$. We shall be interested in determining if our Monte Carlo studies of the pure Baxter-Wu model are in agreement with the series-expansion conjectures, as well as determining the effects of the quenched, random site impurities on the critical exponents and critical amplitudes.

Real-space renormalization-group methods have^{24,25} also been used to study the pure Baxter-Wu model, and the critical eigenvalues obtained give critical exponents consistent with series-expansion and exact results. These studies also give evidence for a third relevant eigenvalue which Barber has shown²⁶ is required from corrections to the asymptotic power-law behavior. The Baxter-Wu model is expected to be in the same universality class as the four-state Potts model. However a Monte Carlo renormalization-group study of the four-state Potts model exhibited²⁷ slow convergence to the fixed point, which was interpreted as evidence for a logarithmic correction to scaling, while a similar study of the pure Baxter-Wu model displayed²⁸ no evidence of logarithmic corrections, in agreement with the exact results.²⁰

We used an importance-sampling Monte Carlo method which has been described elsewhere²⁹⁻³¹ to study the Baxter-Wu model on $L \times L$ triangular lattices with periodic boundary conditions. The lattices used ranged from $L = 6$ to 66 and were chosen so all four ground states of the infinite lattice would fit on the finite lattice without the presence of a misfit seam when periodic boundary conditions were applied. Both a magnetic and a polarization order parameter were included in our study. We defined the magnetic order parameter m as the rms average of the magnetization on the three sublattices. The polarization order parameter p was defined as the rms average of the two-spin correlation functions for nearest-neighbor spins between different sublattices. The rms average rather than the average of the absolute values of the sublattice magnetizations was used because the susceptibilities calculated using the rms average gave results that were in closer agreement with high- and low-temperature series-expansion

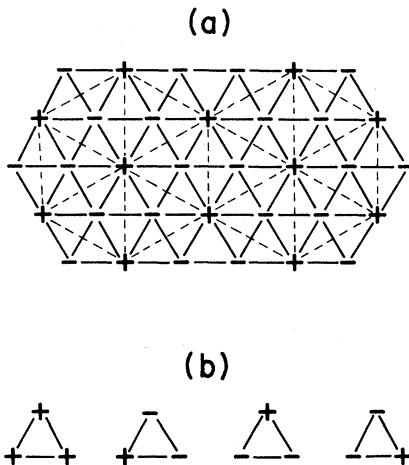


FIG. 1. (a) Shows one of the ferrimagnetic ground states of the Baxter-Wu model. The light dotted line indicates one of the three triangular sublattices of the original triangular lattice. (b) Shows the spin arrangements on a given nearest-neighbor triangle for the ferromagnetic ground state and the three different ferrimagnetic ground states of the Baxter-Wu model.

results. This was attributed to the lack of cross terms caused by the averaging procedure when the expectation value of the square of the order parameter (which is required for the susceptibility) is calculated. These cross terms decrease in importance as L and T increase. The critical exponents calculated using finite-size scaling for either definition are compatible; however, for a given lattice size finite-size scaling is satisfied further from T_c for susceptibilities calculated from rms averages than those from the average of the absolute values of the sublattice magnetization.

Since α is large for the Baxter-Wu model, the fluctuation-dissipation relations require the thermal fluctuations near T_c to be large. Since these fluctuations were found to have a very low frequency, the thermal average of the square of the total internal energy $\langle E^2 \rangle$ had to be averaged over a number of initial spin configurations for each distribution of quenched impurities. This average for different starting spin configurations had to be performed before the specific heat $C/R = (\langle E^2 \rangle - \langle E \rangle^2)/T^2$ was calculated in order to obtain an adequate sample of phase space. Our calculations included at least 8000 MCS (Monte Carlo spin-flip trials per spin) for at least four different starting spin configurations.

The fraction of random, quenched, nonmagnetic site impurities ranged from $x = 0.0$ to 0.444 and was chosen to give an integral number of impurities on all lattice sizes studied. For the impure systems the thermal quantities of interest were calculated for each distribution of quenched site impurities and then averaged over at least four different distributions. Near $T_c(x)$ the values of some thermal quantities varied substantially for each quenched distribution, so we included up to ten different impurity distributions in the configurational averages.

B. Finite-size scaling theory

In order to extract the critical exponents and amplitudes from the data, we have used finite-size scaling theory.^{29,30,32} According to this theory the free energy of an $L \times L$ lattice is given by the scaling ansatz

$$F(L, T) = L^{-\psi} \mathfrak{F}^0(L^\theta t) , \quad (2)$$

where $\psi = (2 - \alpha)/\nu$, $t = |1 - T/T_c(\infty)|$, $T_c(\infty)$ is the infinite-lattice transition temperature, and \mathfrak{F}^0 is a scaling function involving the scaled variable $y = L^\theta t$. The scaling of the correlation length $\xi = \xi_0 t^{-\nu}$ suggests $\theta = 1/\nu$. The scaling of the free energy leads to similar relations for the order parameters m and p , their susceptibilities χ , and the specific heat C of sys-

tems with periodic boundary conditions

$$m = L^{-\beta_m/\nu} X_m^0(y) , \quad (3a)$$

$$p = L^{-\beta_p/\nu} X_p^0(y) , \quad (3b)$$

$$\chi T = L^{\gamma/\nu} Y^0(y) , \quad (3c)$$

$$C - b = L^{\alpha/\nu} Z^0(y) . \quad (3d)$$

Here $y = L^{1/\nu} t$ and b is the nonsingular term of the specific heat. For large y with $L \rightarrow \infty$ and $t \ll 1$ Eqs. (4a)–(4d) must asymptotically reproduce the infinite-lattice critical behavior. Hence in this limit

$$X_m^0(y) \approx B_m y^{\beta_m} , \quad (4a)$$

$$X_p^0(y) \approx B_p y^{\beta_p} , \quad (4b)$$

$$Y^0(y) \approx C^\pm y^{-\gamma} , \quad (4c)$$

$$Z^0(y) \approx A^\pm y^{-\alpha} , \quad (4d)$$

where B_m , B_p , C^\pm , and A^\pm are the critical amplitudes. Also for $T > T_c(\infty)$ the finite-size tails of the order parameters must scale as

$$X_m^0(y) \approx B'_m y^{\beta_m - \nu} , \quad (5a)$$

$$X_p^0(y) \approx B'_p y^{\beta_p - \nu} . \quad (5b)$$

Finite-size scaling can also give the exponent α by using the relation that the maximum specific heat as $L \rightarrow \infty$ must scale as

$$C_{\max}/R \sim L^{\alpha/\nu} + b , \quad (6)$$

where b is the nonsingular term in the specific heat. If $\alpha \geq 0$ then b should be important only for small L .

C. Percolation

For the Baxter-Wu model with random, quenched site impurities we have also determined the impurity concentration x_c above which the infinite lattice has no infinite cluster (and hence cannot possess long-range order for any infinite temperature). This percolation limit was found by randomly distributing a certain fraction of spins on various lattice sizes ranging from $L = 30$ to 180 for 40 different distributions. For a model with two-body interactions (e.g., the Ising model) a cluster is composed of those spins that are connected by a sequence of bonds (lines) that join two nearest-neighbor (NN) spins. For the Baxter-Wu model a cluster consists of those spins that are connected by a sequence of three-body bonds (triangles) that join three spins which are all NN. Hence if two NN spins have no spins which are NN to both they must belong to the same cluster in an Ising model but may not belong to the same cluster in the Baxter-Wu model. The largest cluster for each

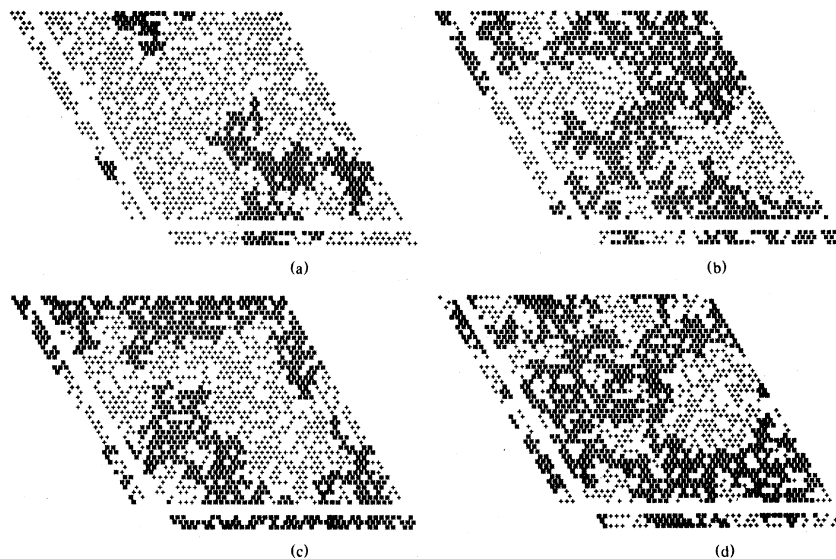


FIG. 2. Sample lattices used in the determination of the percolation limit with $L = 42$ and $x = 0.315$. The spins belonging to the largest cluster (*) and to other clusters (+) are displayed while impurities are left blank. The lattices have the largest cluster: (a) not close to spanning the lattice; (b) close but not quite spanning the lattice in any direction; (c) spanning in one direction only; and (d) spanning in two directions. The disjoint border sections indicate the periodic boundary conditions by showing the next three rows of spins to the left and at the bottom of the lattice. These rows are copied from the right and top of the lattice, respectively.

distribution was then found using a cluster multiple labeling technique,³³ and the entire lattice was plotted. By examining the largest cluster of the lattices, we determined whether the largest cluster spanned the lattice in zero, one, or two directions (see Fig. 2). (That is, we determined whether the largest cluster was topologically similar to a point, a circle, or a torus.) The infinite-lattice percolation limit $p_c = 1 - x_c$ was then determined by extrapolating the concentration of impurities needed to provide a “critical cluster” (one that spanned the lattice) half the time as a function of L^{-1/ν_p} where ν_p is the critical exponent in percolation that describes the divergence of the connectivity length $\xi(x) \propto |x - x_c|^{-\nu_p}$. In two dimensions $\nu_p \approx 1.35$.³⁴ The extrapolations were performed both with and without the clusters that spanned the lattice in only one direction being encompassed by the definition of a “critical cluster.” The percolation limit could be more accurately determined using finite-size scaling for various cluster sizes,³⁴ but this would require the use of lattices having about two orders of magnitude more lattice sites³⁵ than used in our study.

III. RESULTS

A. Thermal properties

In order to obtain good quality data, it was necessary to use a large number of MCS for a number of

different starting configurations for each temperature, lattice size, and impurity distribution. This was not only because the thermal fluctuations were large (α is large) but also because the time scale for such fluctuations was long. These low-frequency fluctuations are evident in Fig. 3 which shows the internal energy as a function of time for a single starting configuration. From a comparison of the upper and lower portions of Fig. 3 we see that the low-frequency fluctuations are due to the motion and growth of domain boundaries. Similar low-frequency fluctuations were also observed in the simulation when random, quenched, site impurities were added to the system. In fact, the impurities tended to “pin” the boundary between various domains making the fluctuations due to the movement of domains extremely long. If we looked at only the first 2000 MCS in Fig. 3 it appeared that the system was in a metastable state. (2500 MCS were thrown away in order for the system to reach thermal equilibrium from a ferromagnetic ground state before the start of the internal energy plot in Fig. 3.) This would normally indicate a first-order transition. However, looking at the entire number of MCS it is apparent that the system has very large fluctuations at both high and low frequencies and hence the behavior is indeed characteristic of a second-order transition. (For the pure lattice it is known exactly²⁰ that the transition is second order.)

The internal energy as a function of temperature is shown in Fig. 4 for various lattice sizes and impurity

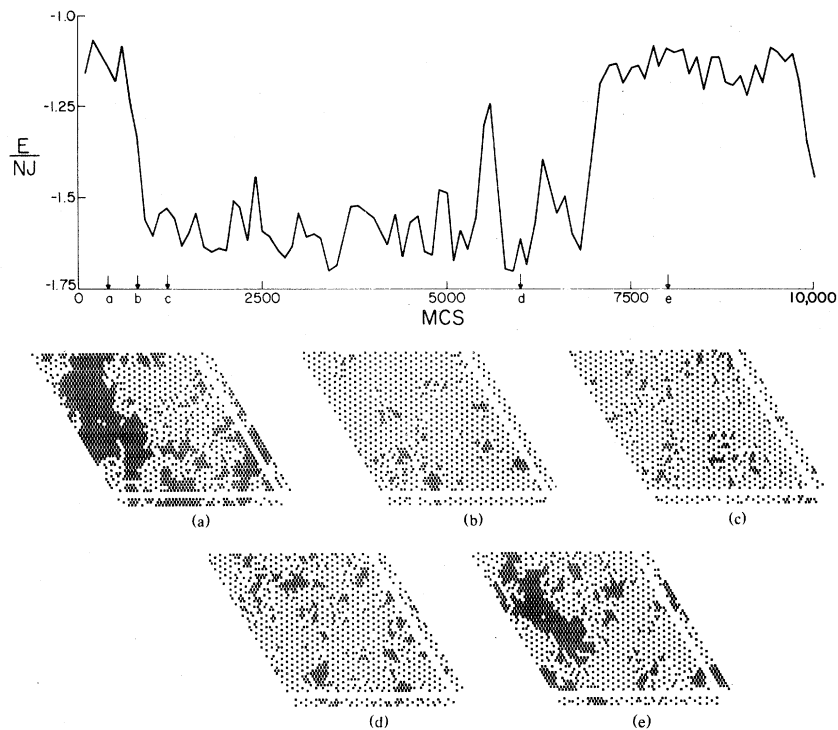


FIG. 3. Internal energy as a function of MCS is shown for a single starting configuration on a pure ($x=0$) 48×48 lattice at $kT/J = 2.2775$. The arrows indicate the points where the spin configuration is shown. Up spins are indicated by * and down spins by blanks. The disjoint border sections indicate the periodic boundary conditions by showing the next three rows of spins to the right and at the bottom of the lattice. These rows are copied from the top and right of the lattice, respectively.

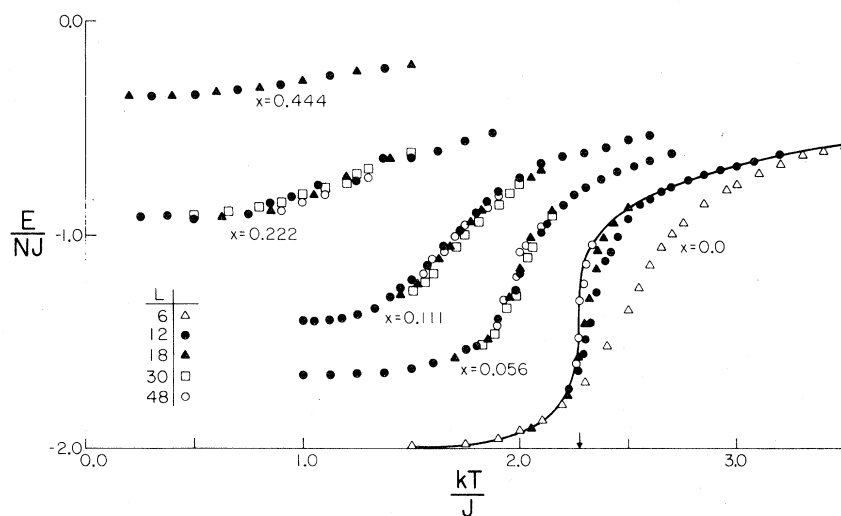


FIG. 4. The internal energy is plotted as a function of temperature for various impurity concentrations and lattice sizes. The arrow indicates the pure lattice critical temperature while the solid line is the exact internal energy for the pure lattice from Ref. 20.

concentrations. Note that these data as well as those in the following figures are plotted per lattice site and not per magnetic site. As the impurity concentration increases the inflection points (which correspond to the maximum in the specific heat) shift to lower temperatures and the ground-state internal energy approaches zero. The finite-size effects are important only near $T_c(x)$ and are clearly much more pronounced near $x=0$ than for the impure systems. Note that $x=0.444$ is below the percolation limit and hence no transition can occur.

Figure 5 shows the specific heat as a function of temperature for various lattice sizes and impurity concentrations. For the pure lattice the specific heat maximum increases with the lattice size. Also as L increases the width of the specific heat decreases and its position shifts down toward the $L = \infty$ transition temperature. The effects of the addition of random, quenched, site impurities are very striking! The height of the specific heat peak is now virtually independent of L for the larger lattice sizes. Also the width and position of the specific heat maximum for a given impurity concentration is independent of L within the errors of the data. Note that as the impurity concentration increases the height of the specific heat peak decreases, its width increases, and the temperature at which the specific heat peak has its maximum decreases.

The phase diagram for the impure Baxter-Wu model, found assuming the specific heat maxima indicate the critical temperatures, is shown in Fig. 6. Note that $T_c(x)/T_c(x=0)$ decreases more rapidly as x increases for the Baxter-Wu model than for the standard two-dimensional Ising model. Whether the specific heat maxima give the true critical temperature will be discussed in Sec. IV B.

B. Order-parameter properties

The behavior of both the magnetic and polarization order parameters are shown in Fig. 7 for several impurity concentrations. Both order parameters in all cases show a rapid decrease near the maxima of the specific heat peak, and finite-size "tails" at higher temperatures. Owing to our normalization, at low temperatures the magnetic order parameter m tends to $1-x$ rather than to unity. The value to which the polarization order parameter p tends as $T \rightarrow 0$ depends on the particular quenched distribution since the number of nearest-neighbor spins varies for different distributions. For large L (or averaging over enough distributions) as $T \rightarrow 0$ p tends toward $(1-x)^2$ since the probability that both spins of a nearest-neighbor pair are present is the square of the probability that a given spin is present. The data in-

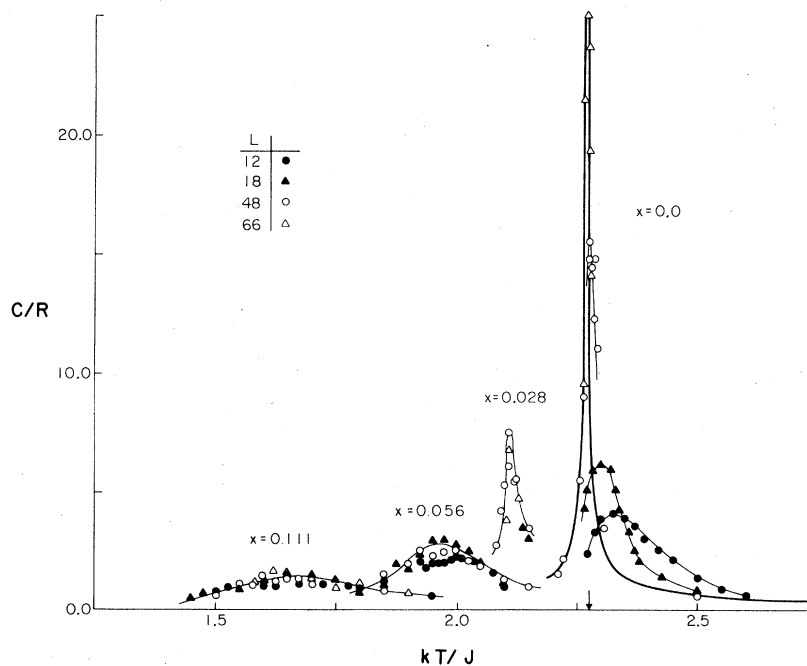


FIG. 5. The specific heat is plotted as a function of temperature for various lattice sizes and impurity concentrations. The arrow indicates the pure lattice critical temperature and the heavy line the exact specific heat for the pure lattice from Ref. 20. The light lines are to be used as guides for the eye.

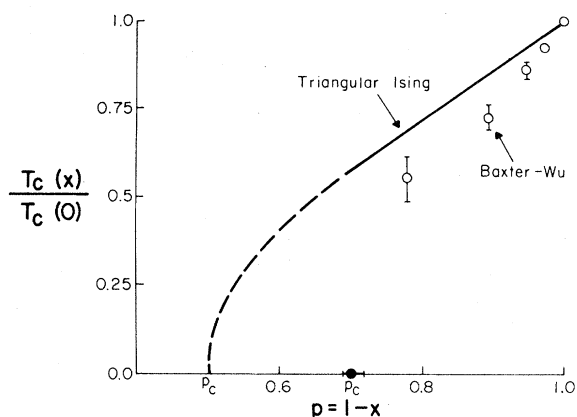


FIG. 6. Dependence of T_c on the purity concentration $p = 1 - x$. The open circles are Monte Carlo results and the closed circle is our percolation estimate. The solid curve is for the triangular Ising model (Refs. 16–18) for which $p_c = 0.5$ exactly (Ref. 36).

dicating that for all values of x (if the same normalization for m and p were used) near $T_c(x)$ the magnetic order parameter m is slightly larger than the polarization order parameter. If $\beta_m = \beta_p$ this suggests that the critical amplitudes satisfy $B_m > B_p$. Our data for $x = 0$ follow the conjectured²³ “exact results” obtained from the study of low-temperature series which give $B_m/B_p = 3/2\sqrt{2}$.

Figure 8 shows the zero-field susceptibilities for the two order parameters for various lattice sizes and impurity concentrations. The susceptibilities obtained for the pure model compare favorably for temperatures far from $T_c(\infty)$ with low-temperature^{22,23} and high-temperature³⁷ series expansions. For $x = 0$ the maximum value of the susceptibility increases markedly as L increases, while the width of the maximum decreases and the temperature at which the maximum occurs shifts down toward the infinite-lattice transition temperature. The effect of the quenched impurities for a given lattice size is to decrease the maximum height, increase the width, and lower the temperature at which the maximum occurs.

IV. ANALYSIS AND DISCUSSION

A. Pure-model critical behavior

Figure 9 shows a finite-size scaling plot for the pure lattice specific heat using the exact values²⁰ of T_c , α , ν , and b with no adjustable parameters. This graph shows that finite-size scaling is applicable to the Baxter-Wu model and gives the form of $Z^0(y)$ in Eq. (3d). Note that $Z^0(y)$ is not a symmetric function of y and for $T > T_c$ approaches the asymptotic region only for very large values of y . Figure 10 shows the finite-size scaling plots for the two order parameters using the exact values for ν and T_c and $\beta_m = \beta_p = \frac{1}{12}$. The critical amplitudes for the order parameters from the finite-size scaling plots are

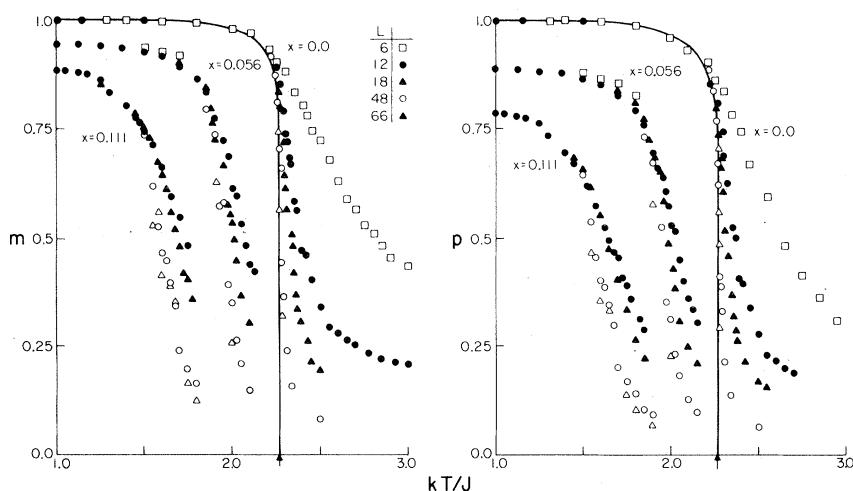


FIG. 7. The magnetic and polarization order parameters are shown as a function of temperature for various lattice sizes and impurity concentrations. The arrows indicate the pure lattice critical temperature from Ref. 20, and the heavy lines indicate the conjectures for the exact spontaneous magnetization and spontaneous polarization from the low-temperature series of Ref. 23.

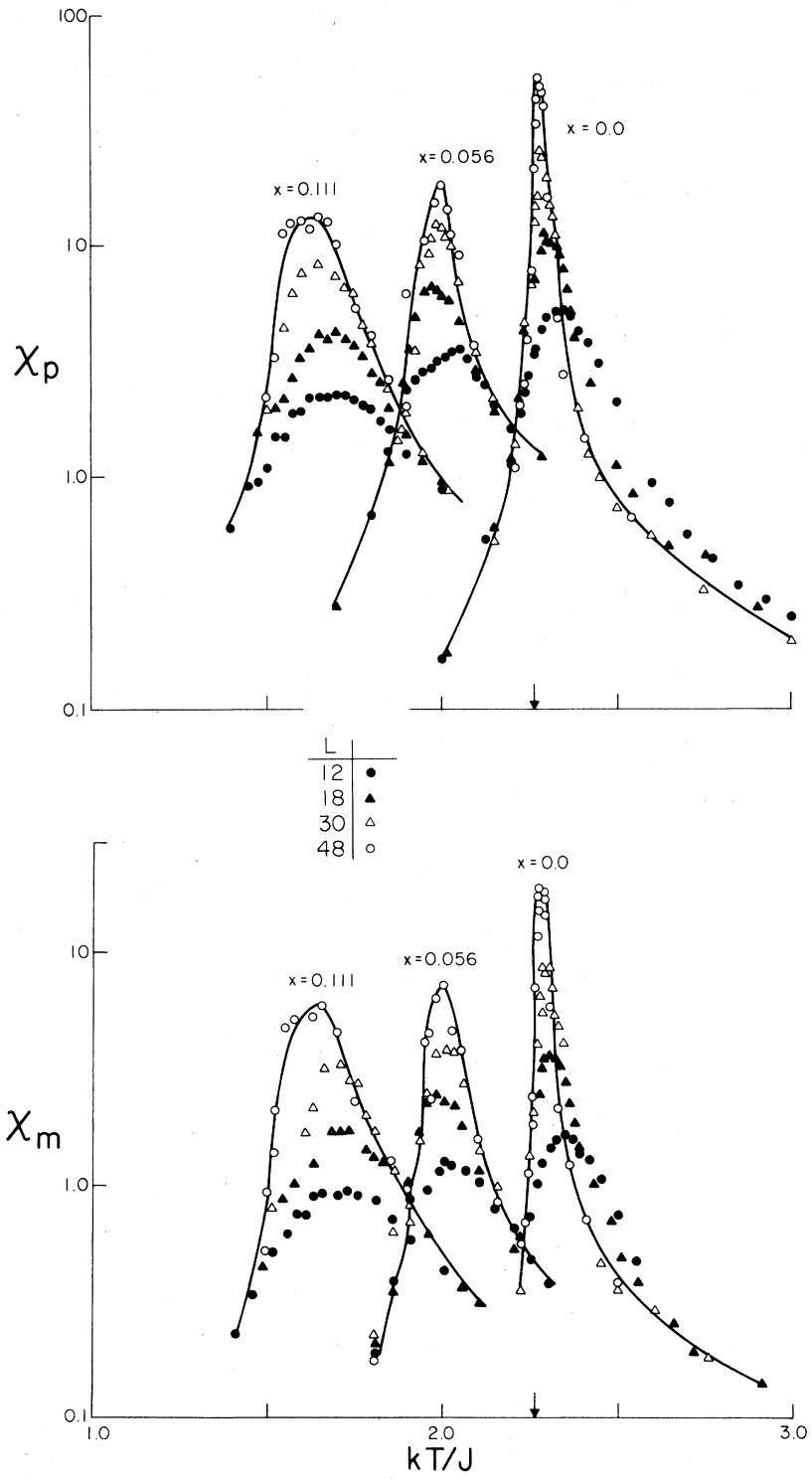


FIG. 8. The zero-field susceptibility for the magnetization and polarization order parameters are shown as a function of temperature for various lattice size and impurity distributions. The arrow indicates the infinite lattice T_c for $x = 0$.

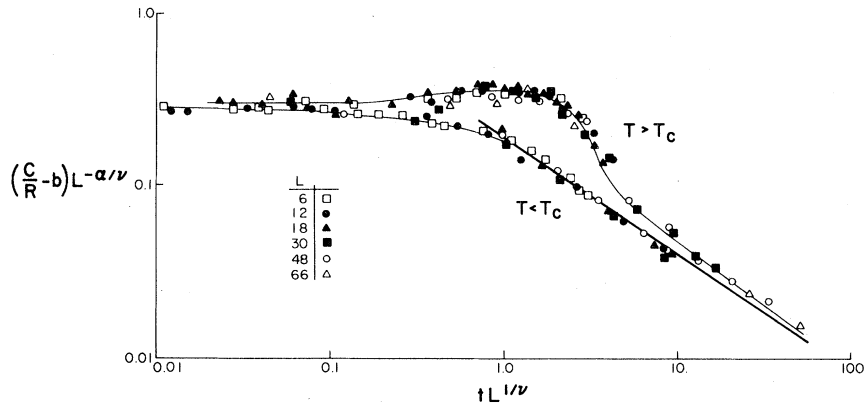


FIG. 9. Finite-size scaling plot for the divergent part of the specific heat of the pure Baxter-Wu model using the known values of T_c , α , ν , and b . The heavy line is the exact asymptotic form from Ref. 20. The light lines are to be used as guides for the eye.

$B_m = B_p = 1.2 \pm 0.1$. Figure 11 shows the finite size scaling plots for the reduced zero field susceptibility for both order parameters when $T > T_c$; the plot uses the exact values of T_c and ν together with the low-temperature series estimate (with $\gamma = \gamma'$) of $\gamma_m = \gamma_p = 1.17$. The scaling parameter used is $L^{1/\nu} t'$ where $t' = 1 - T_c/T$. A similar plot for data with $T < T_c$ was consistent with the low-temperature series²³ estimates of $\gamma'_m = \gamma'_p = 1.17$. Since $\beta_m = \beta_p$ one expects from scaling relations that $\gamma'_m = \gamma'_p$, and the data confirm this. Because the scaling function $Y^0(y)$ approaches the asymptotic limit only for large y (and large L) the critical amplitudes could not be

determined very precisely: $C_m^- = 0.01 \pm 0.005$, $C_m^+ = 0.03 \pm 0.02$ and $C_p^- = 0.04 \pm 0.02$, $C_p^+ = 0.06 \pm 0.03$. Note the asymptotic form for all scaling functions was reached only for $y \geq 10$ in contrast to the 2D and 3D Ising model studies where the asymptotic limits were reached for $y \geq 2$.

B. Percolation limit

The extrapolation of the percolation data to obtain the infinite-lattice percolation limit is shown in Fig. 12. The value obtained for the percolation limit is $p_c = 1 - x_c = 0.71 (+0.02, -0.01)$ and is independent

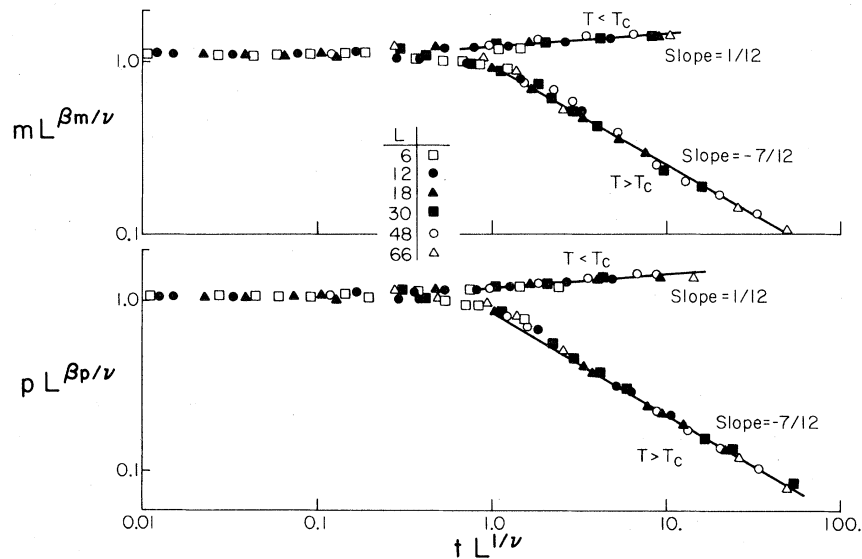


FIG. 10. Finite-size scaling plots for the two order parameters of the pure lattice using the exact values of ν and T_c and $\beta_m = \beta_p = \frac{1}{12}$.

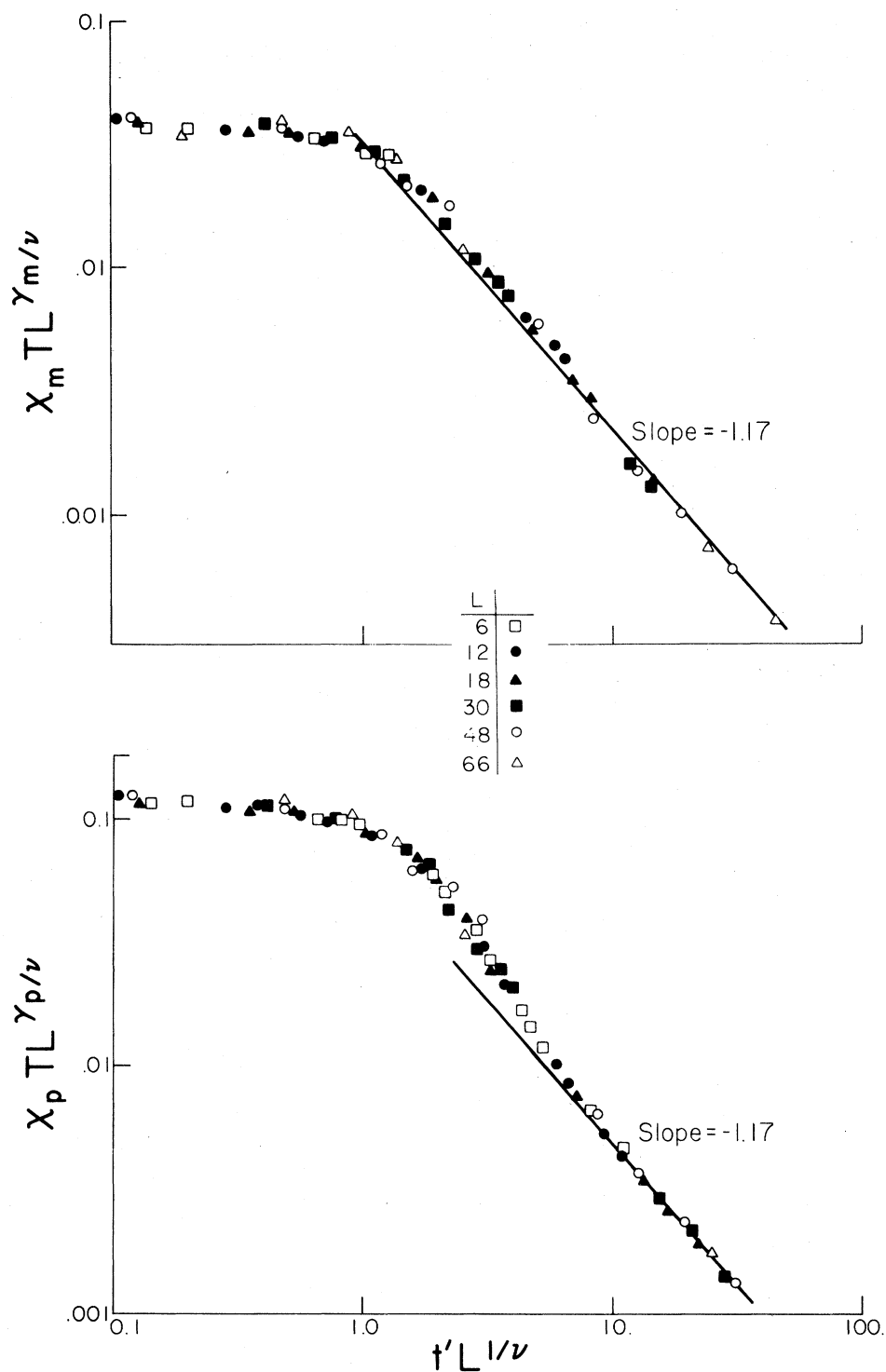


FIG. 11. Finite-size scaling plots for the pure lattice zero-field reduced magnetic and polarization susceptibilities are shown for $T > T_c$ using the exact values of T_c and ν with $\gamma_m = \gamma_p = 1.17$. The solid lines give $C_m^+ = 0.03$ and $C_p^+ = 0.06$.

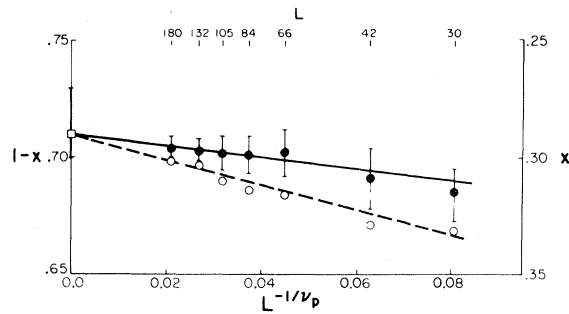


FIG. 12. The extrapolation of the infinite-lattice percolation from the "critical clusters" of finite lattices is shown. The filled circles and heavy line are for "critical clusters" that span the lattice in two directions. The open circles and dotted line are for "critical clusters" that span the lattice in either one or two directions. The error estimates for the open circles are comparable to those of the closed circle, but are not indicated in the figure.

of whether or not clusters that spanned the lattice in only one direction were counted as "critical clusters." The upper bound on our percolation estimate assumes that the lattices studied were of sufficient size that a straight line fit through the data would extrapolate to the infinite-lattice percolation limit. A recent study³⁸ has been done of the Baxter-Wu model with annealed bond impurities by mapping it onto the pure Baxter-Wu model. This study assumed that the ratio of p_c for annealed bond impurities and p_c for quenched site impurities is a function only of the lattice not of the spin Hamiltonian. Using this to compare the Baxter-Wu model and the triangular Ising model they predicted $p_c \sim 0.71$ for the Baxter-Wu model with quenched site impurities.

C. Impure-model critical behavior

Determining the critical temperature $T_c(x)$ for an impure system is nontrivial. Real-space renormalization-group studies¹⁵ of bond-impure models as well as experimental results on physical systems³⁹ suggest that the specific heat anomaly associated with long-range order may become a very narrow cusp superimposed on the low-temperature shoulder of a broad peak produced by short-range order. Figure 7 shows that both order parameters exhibit a rapid decrease in magnitude near where the specific heat peak maxima occur. Figure 8 demonstrates that both susceptibilities have a maximum where the corresponding maximum of the specific heat peak occur. In addition finite-size scaling plots using the critical temperature given by the specific heat maximum show the data for the two order parameters and their corresponding susceptibilities scale very well. This evidence implies that if there is a cusp in the infinite-lattice specific

heat it must be located within our error estimates for the specific heat maxima. This provides the justification for using the specific heat maxima to locate the critical temperature as a function of impurity concentration as was done in the phase diagram shown in Fig. 6.

The dramatic change in the specific heat with the addition of quenched site impurities is demonstrated in the finite-size scaling plot for the maximum specific heat in Fig. 13. For the pure Baxter-Wu model ($x=0$) all points with $L \geq 18$ fall on a line with slope $\alpha/\nu = 1.0$; if the exact²⁰ nondivergent part of the specific heat $b = -2(J/kT_c)^2 \approx 0.388$ had been subtracted from the specific heat maximum the points for $L=6$ and 12 of the pure lattice would also lie on the line in the figure. Figure 13 indicates that the addition of impurities changes the ratio of α/ν from unity to close to zero! Hence $\alpha \leq 0$ for all impurity concentrations studies from $x=0.027$ to the percolation limit. Note the smaller the impurity concentration x the larger the lattice one must simulate to find the "impure" ratio $\alpha/\nu \approx 0$. This indicates that for a finite lattice the true asymptotic behavior is observed only when its specific heat maximum is within some "impure critical region" around the infinite-lattice transition temperature. This is consistent with the prediction⁷ that the width of the "impure critical region" increases with the impurity concentration. Very detailed data were obtained for $x=0.111$ for which the modified behavior occurs over a wide range of lattice sizes. The crossover in critical exponents with the addition of quenched impurities is also clearly observed in other exponents as shown in Fig. 14. The figure shows two finite-size

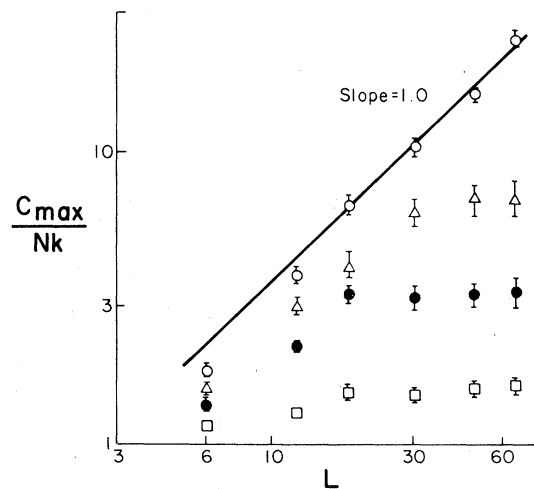


FIG. 13. Maximum specific heat as a function of lattice size is plotted for $x=0.0$ (\circ), $x=0.028$ (Δ), $x=0.056$ (\bullet), and $x=0.111$ (\square). The line drawn through the pure model data has a slope equal to $\alpha/\nu = 1.0$.

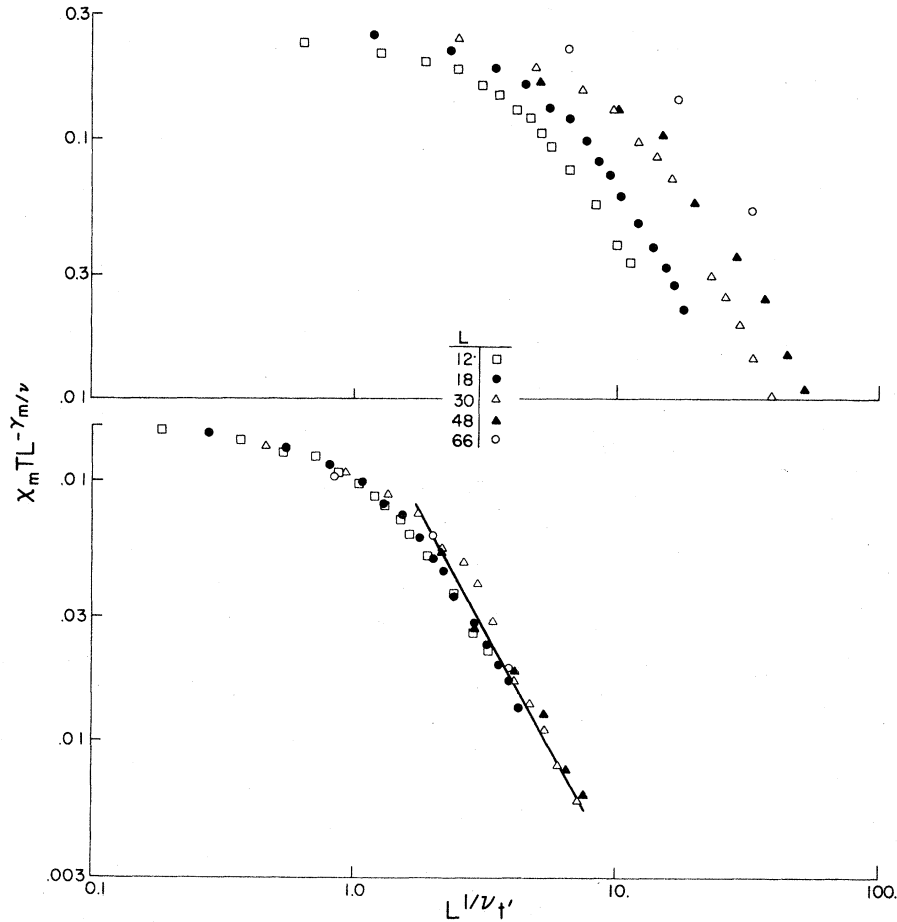


FIG. 14. The scaled zero-field susceptibility for $x=0.111$ and $T > T_c$ is shown using $kT_c/J=1.60$. The top graph uses the pure lattice exponents ($\nu = \frac{2}{3}$, $\gamma_m = 1.17$). The bottom graph uses $\nu = 1.0$ and $\gamma_m = 1.95$.

scaling plots for the zero-field magnetic susceptibility using $kT_c/J = 1.6$ (obtained from the specific heat maximum). Using the pure lattice critical exponents ($\nu = \frac{2}{3}$, $\gamma_m = 1.17$) we found that the data did not scale as Fig. 14(a) demonstrates. Figure 14(b) shows that the data scale well using $\nu = 1.0$ and $\gamma_m = 1.95$. Thus a dramatic change in γ_m is caused by the addition of the quenched impurities. Using $\nu = 1.0$ and $\gamma_p = 1.95$ gives a good scaling plot for the zero-field polarization susceptibility. Scaling plots for the data with $T < T_c$ gave critical exponents consistent with the values obtained for the data with $T > T_c$.

For the magnetic and polarization order parameters the data for $x=0.111$ scaled well using $kT_c/J=1.6$ with $\nu = 1.0$ and $\beta_m = \beta_p = 0.12$. However because of the small values of β the error estimates for β_m and β_p for $x=0.111$ were large and encompass the pure model values. To be able to clearly show any crossover in the order-parameter critical exponents one

would have to study very large lattices near T_c and an extremely large number of MCS would be needed.

V. SUMMARY AND CONCLUSIONS

The results of our Monte Carlo study describe the behavior of the pure Baxter-Wu model and the Baxter-Wu model with random, quenched, nonmagnetic, site impurities. The alteration of the critical exponents with the addition of quenched site impurities is very pronounced. This modified critical behavior with the addition of quenched impurities could only be seen within some "impure critical region" around the critical temperature. This region increases in size as the impurity concentration is increased in a manner consistent with the prediction by Harris.⁷ Upon the addition of the quenched impurities α changes from the pure lattice value of $\frac{2}{3}$ to

0.0 ± 0.2 while ν changes from $\frac{2}{3}$ to 1.00 ± 0.07 . The susceptibility exponents for the spontaneous magnetization and spontaneous polarization change from the pure value of $\gamma_m \approx \gamma_p \approx 1.17$ to $\gamma_m \approx \gamma_p \approx 1.95 \pm 0.08$. No change in the critical exponents β_m and β_p could be detected for the lattice sizes studied. The observed crossover in the critical exponents substantiates the conjecture by Harris⁷ of the effect random, quenched impurities have on a system with $\alpha > 0$. The inability to observe such crossover of the critical exponents in previous Monte Carlo studies¹⁹ for the simple cubic Ising model ($\alpha \approx \frac{1}{8}$) can be attributed to the required use of extremely large lattices in order to penetrate the "impure critical region." The maximum specific heat as a function of impurity concentration is shown in Fig. 15. Harris has predicted that $C_{\max}/R \sim 1/x$ for small x , and the data are consistent with this hypothesis.

The exponents for both the pure and the impure Baxter-Wu model obey scaling, hyperscaling,⁴⁰ and Suzuki weak universality⁴¹ within the error estimates. The impure critical exponents appear to have the same value for all impurity concentrations studied from $x = 0.028$ to 0.222 . This suggests that the addition of quenched impurities causes the Baxter-Wu fixed point to become unstable and another fixed point to become stable. From this study we cannot determine whether the new stable fixed point is the fixed point associated with the pure 2D Ising model or an "impure fixed point." Renormalization-group work using ϵ expansions⁹⁻¹⁴ suggest that the stable fixed point is an "impure fixed point." A recent Monte Carlo renormalization-group study⁴² of the Baxter-Wu "impure fixed point" has suggested that Suzuki weak universality may not hold for the critical exponent δ of the impure system. It is not obvious that Suzuki weak universality should be rigorously sa-

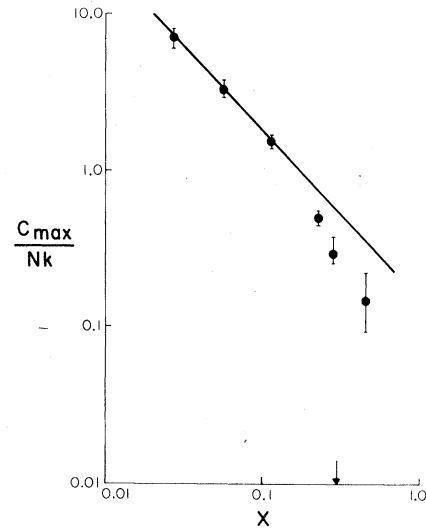


FIG. 15. The maximum specific heat as a function of impurity concentration is plotted. The arrow shows the percolation limit. The line has a slope equal to -1 .

tified for all models since Baxter⁴³ has recently obtained an exact solution to a two-dimensional model that violates Suzuki weak universality. If Suzuki weak universality does not hold for the impure Baxter-Wu model then the new stable fixed point must be an "impure fixed point."

ACKNOWLEDGMENTS

This work was supported in part by the National Science Foundation. The authors wish to thank Dr. E. B. Rasmussen for his suggestions concerning the manuscript.

¹I. Syozi, *Prog. Theor. Phys.* **34**, 189 (1965).

²H. Garelick and J. W. Essam, *Proc. Phys. Soc. London* **92**, 136 (1967).

³M. E. Fisher and H. Au Yang, *J. Phys. C* **8**, L418 (1975); H. Au Yang and M. E. Fisher, *Phys. Rev. B* **13**, 1238 (1976); **13**, 1266 (1976).

⁴B. M. McCoy and T. T. Wu, *Phys. Rev.* **176**, 631 (1968); B. M. McCoy and T. T. Wu, *The Two-Dimensional Ising Model* (Harvard University Press, Cambridge, Mass., 1973), Chaps. XIV and XV.

⁵G. S. Rushbrooke and D. J. Morgan, *Mol. Phys.* **4**, 1 (1961); D. J. Morgan and G. S. Rushbrooke, *ibid.* **4**, 291 (1961); **6**, 477 (1963).

⁶R. J. Elliot and B. R. Heap, *Proc. R. Soc. London Ser. A* **265**, 264 (1962).

⁷A. B. Harris, *J. Phys. C* **7**, 1671 (1974).

⁸Although Harris worked with systems having random bond impurities, his analysis should also hold for systems with random site impurities.

⁹A. B. Harris and T. C. Lubensky, *Phys. Rev. Lett.* **33**, 1540 (1974).

¹⁰T. C. Lubensky, *Phys. Rev. B* **11**, 3573 (1975).

¹¹D. E. Khmel'nitskii, *JETP* **41**, 981 (1976).

¹²G. Grinstein and A. Luther, *Phys. Rev. B* **13**, 1329 (1976).

¹³A. Aharony, Y. Imry, and S.-K. Ma, *Phys. Rev. B* **13**, 466 (1976).

¹⁴C. Jayaprakash and H. J. Katz, *Phys. Rev. B* **16**, 3987 (1977).

¹⁵C. Jayaprakash, E. K. Riedel, and M. Wortis, *Phys. Rev. B* **18**, 2244 (1978).

¹⁶W. Y. Ching and D. L. Huber, *Phys. Rev. B* **13**, 2962 (1976).

- ¹⁷E. Stoll and T. Schneider, in *Magnetism and Magnetic Materials—1975*, edited by J. J. Becker, G. H. Lander, and J. J. Rhyne, AIP Conf. Proc. No. 29 (AIP, New York, 1976), p. 490.
- ¹⁸R. Fisch and A. B. Harris, in *Magnetism and Magnetic Materials—1975*, edited by J. J. Becker, G. H. Lander, and J. J. Rhyne, AIP Conf. Proc. No. 29 (AIP, New York, 1976), p. 488.
- ¹⁹D. P. Landau, *Physica* **86-88B**, 731 (1977); D. P. Landau, *Phys. Rev. B* **22**, 2450 (1980).
- ²⁰R. J. Baxter and F. Y. Wu, *Phys. Rev. Lett.* **31**, 1294 (1973); *Aust. J. Phys.* **27**, 357 (1974); R. J. Baxter, *ibid.* **27**, 368 (1974).
- ²¹M. A. Novotny and D. P. Landau, *J. Magn. Magn. Mater.* **15-18**, 247 (1980).
- ²²H. P. Griffiths and D. W. Wood, *J. Phys. C* **6**, 2533 (1973); D. W. Wood and H. P. Griffiths, *ibid.* **7**, 1417 (1974).
- ²³M. G. Watts, *J. Phys. A* **7**, L85 (1974); M. F. Sykes and M. G. Watts, *ibid.* **8**, 1469 (1975); R. J. Baxter, M. F. Sykes, and M. G. Watts, *ibid.* **8**, 245 (1975).
- ²⁴H. J. Braathen and P. C. Hemmer, *Phys. Norv.* **8**, 69 (1975); D. Imbro and P. C. Hemmer, *Phys. Lett.* **57A**, 297 (1976).
- ²⁵M. P. M. den Nijs, A. M. M. Pruisken, and J. M. J. van Leeuwen, *Physica* **84A**, 539 (1976).
- ²⁶M. N. Barber, *J. Phys. A* **9**, L171 (1976).
- ²⁷C. Rebbi and R. H. Swendsen, *Phys. Rev. B* **21**, 4094 (1980).
- ²⁸M. A. Novotny, D. P. Landau, and R. H. Swendsen (unpublished).
- ²⁹D. P. Landau, *Phys. Rev. B* **13**, 2997 (1976).
- ³⁰D. P. Landau, *Phys. Rev. B* **14**, 255 (1976).
- ³¹For a general review see "Monte Carlo Methods" in *Statistical Physics*, edited by K. Binder (Springer, Berlin, 1979).
- ³²M. E. Fisher, in *Proceedings of the International Summer School "Enrico Fermi", Course LI, 1970*, edited by M. S. Green (Academic, New York, 1971).
- ³³J. Hoshen and R. Kopelman, *Phys. Rev. B* **14**, 3438 (1976).
- ³⁴D. Stauffer, *Phys. Rep.* **54**, 1 (1979), and references cited therein.
- ³⁵J. Hoshen, D. Stauffer, G. H. Bishop, R. J. Harrison, and G. D. Quinn, *J. Phys. A* **8**, 1285 (1979).
- ³⁶M. F. Sykes and J. F. Essam, *Phys. Rev. Lett.* **10**, 3 (1963).
- ³⁷D. W. Wood and H. P. Griffiths, *J. Math. Phys.* **14**, 1715 (1973).
- ³⁸A. R. McGurn and R. A. Tahir-Kheli, *Phys. Status Solidi B* (in press).
- ³⁹M. A. Algra, L. J. Jongh, and W. J. Huiskamp, *Physica* **86-88B**, 737 (1979).
- ⁴⁰See, for example, H. E. Stanley, *Introduction to Critical Phenomena and Phase Transitions* (Oxford University Press, New York, 1971).
- ⁴¹M. Suzuki, *Prog. Theor. Phys.* **51**, 1992 (1974).
- ⁴²D. P. Landau and M. A. Novotny, *Physica A* (in press).
- ⁴³R. J. Baxter, *J. Phys. A* **13**, L61 (1980).